Journal of Ecology of Health & Environment
*An International Journal*

http://dx.doi.org/10.18576/jehe/140101

# An Investigation of the Langevin Equation for Predicting Dispersion from Elevated Point Source in the Convective Boundary Layer

*Khaled S.M. Essa*[1,*], *Ahmed M. Mosallem*[1] *and Fawzia Mubarak*[2].

[1] Mathematics and Theoretical Physics Department, Nuclear Research Center (NRC), Egyptian Atomic Energy Authority, (EAEA), Cairo, Egypt
[2] Nuclear Fuel Cycle Safety Department, Nuclear and Radiological Safety Research Center (NRSRC), Egyptian Atomic Energy Authority (EAEA), Cairo, Egypt

Received: 5 Sep. 2025, Revised: 25 Oct. 2025, Accepted: 30 Nov. 2025.
Published online: 1 Jan. 2026

**Abstract:** The following are explained: E-ε Model, E-l Model, Parameterized Length Scale Model, Parameterization of Turbulent Transport, Parameterization of Dissipation, Parameterization of Return-to-Isotropy Terms, Subgrid-scale models, Lagrangian Stochastic Models, Random-walk Model for Homogeneous Turbulence, Random-walk Model for Inhomogeneous Turbulence, and Short-Range Gradient Transport Models. In this research, the sequential approximation method was used as an alternative numerical method to solve the three-dimensional stochastic Langevin equation. After obtaining Langevin models for Gaussian, a comparison was made between the Copenhagen experimental data of Sulfur Hexafluoride ($SF_6$). The two models are within a factor of two of the observed data, according to statistical assessments and stochastic analysis between the observed and predicted data. Additionally, the Correlation coefficient, Normalized Mean Square Error, and Fraction Bias are all in good agreement with the observed data.

**Keywords:** Langevin equation, vertical turbulence velocity, probability density function, and numerical simulations.

## Abbreviations

Planetary Boundary Layer (PBL)

Probability Density Functions (PDF)

Iterative Langevin Solution (ILS)

Monin Obukhov (M-O)

ground level concentration (g. l. c.)

Turbulence Kinetic Energy (TKE)

large-eddy length scale ($\ell$)

Stably Boundary Layer (SBL)

Convective Boundary Layer (CBL)

Large Eddy Scale (LES)

Buoyancy Flux parameter ( $F_b$)

Sulfur Hexafluoride (SF6)

Normalized Mean Square Error (NMSE)

Fraction Bias (FB)

Correlation (COR)

Factor of Two (FAC2)

Kolmogorov's structure function constant ($c_0$)

The rate of energy dissipation ($\varepsilon$)

## 1. Introduction

Several theories of dispersion in turbulent flows were covered in this paper, along with some analytical models derived from these theories for specific atmospheric dispersion applications. There has been discussion of the different drawbacks of the analytical dispersion models based on constant or changing eddy diffusivities. Despite being widely utilized in regulatory applications, the more straightforward Gaussian dispersion models with empirical dispersion parameters or coefficients have a number of drawbacks and uncertainties [1]. The assumptions of all analytical dispersion models include an idealized (horizontal homogenous and quasi stationary) atmospheric boundary layer and a flat, uniform surface that merely reflects, rather than absorbs, the contaminants that reach it. Most of the simpler models assume constant diffusivities and straight line uniform transport wind however some allow for power law diffusivity and wind profiles. In some of these models, the ad hoc consideration of the limit to vertical diffusion by the capping inversion at the top of the planetary boundary layer (PBL) is taken into account [2-3]. Beyond a downwind distance of around 10 km from a continuous point or line source, these analytical dispersion models would not be useful. These models significantly simplify and parameterize transport and diffusion phenomena, even for shorter distances. Lagrangian stochastic particle models are the greatest option for achieving the atmospheric dispersion approach [4]. It is

*Corresponding author e-mail: mohamedksm56@yahoo.com

assumed that the particle displacements are produced by a Markovian process when random velocities are used. The Langevin equation is based on the theory that a combination of a stochastic and a deterministic term determines velocity [5]. The Langevin equation for Gaussian turbulence conditions is solved using this technique. The initial velocity (at t = 0) is found when the Probability Density Functions (PDF) of the turbulent velocity are Gaussian, the stochastic term of the Langevin equation, where the PDF of the turbulent velocity is represented by the combination of Gaussian, Iterative Langevin Solution (ILS) method is evaluated during the Copenhagen tracer experiment taking into account the values of the ground-level concentration.

Mixed Chebyshev and Legendre polynomials differentiation matrices for solving initial-boundary value problems, Aims Mathematics was developed [6]. Chebyshev polynomial derivative-based spectral tau approach for solving high-order differential equations was studied [7]. Three dimensions nanofluid flow over nonlinearly stretching/shrinking sheet with nonlinear thermal radiation: Novel approximation via Chebyshev polynomials' derivative pseudo-Galerkin method was investigated [8].

This work uses a different numerical method to solve the Langevin equation for the dispersion of air pollution. The Langevin models for Gaussian theoretical and experimental data from Copenhagen were compared.

## 2.Short-Range Gradient Transport Models

In some situations, wind-direction shear can be ignored and one can use two-dimensional grid models for solving the finite-difference version of the cross-wind integrated diffusion equation. The influence of the Coriolis turning of wind with height can be considered only in a fully three-dimensional grid model [9].

## 3.Dispersion in the Surface Layer

The governing steady-state diffusion equation can be numerically solved to simulate the diffusion of falling particles from a cross-wind line source in the stratified surface layer:

$$\bar{u}\frac{\partial \bar{C}}{\partial x} - v_g\frac{\partial \bar{C}}{\partial z} = \frac{\partial}{\partial z}\left(K_z\frac{\partial \bar{C}}{\partial z}\right) \quad (1)$$

where $K_z$ is the vertical eddy diffusivities in the z-direction and $\bar{u}$ is the wind speed profile in the x-direction [10]. It was believed that the lower surface would be a perfect sink with zero particle concentration. Additionally, it was believed that the concentration at the upper barrier, which was selected far above the source height, was zero. For three stability conditions, numerical calculations were performed for two values of the dimensionless terminal fall velocity ($k\, v_g/u_* = 0$ and 0.1), with $z_0/L$ given.

The more suitable reflecting or partially reflecting boundary conditions of the vertical dispersion of passive pollutants from a line source can be used to solve Eq. (1) without the gravitational settling term [11].

$$K_z\frac{\partial \bar{C}}{\partial z} = v_d\bar{C} \qquad \text{for } z \to z_0$$

$$K_z\frac{\partial \bar{C}}{\partial z} = 0 \qquad \text{for } z \to \infty \quad (2)$$

According to the lower boundary condition, the mass flux close to the ground needs to match the rate of deposition. Two different vertical-eddy diffusivity specifications, $K_z = K_h$ and $K_z = 1.35\, K_m$, were employed in Ref. [12]. Empirical Monin-Obukhov (M-O) similarity expressions [1, 13] were used to specify the eddy diffusivities of heat and momentum as well as mean velocity, and numerical solutions were produced for various stability factors.

### 3.1.Dispersion in the Planetary Boundary Layer

The dispersion from a continuous point source in the PBL with varying wind and diffusivity profiles was studied using a numerical model by ref. [14]. The Coriolis twisting of the wind was disregarded, and they believed that along-wind diffusion was insignificant compared to advection. The finite-difference variant of the steady-state mean diffusion equation was solved for an elevated point source:

$$\bar{u}\frac{\partial \bar{C}}{\partial x} = \frac{\partial}{\partial y}\left(K_y\frac{\partial \bar{C}}{\partial y}\right) + \frac{\partial}{\partial z}\left(K_z\frac{\partial \bar{C}}{\partial z}\right) \quad (3)$$

which, specified $\bar{u}, K_y$ and $K_z$ as functions of "z" and additional factors (such as mixing height, surface roughness, surface heat flow, and geostrophic wind speed). According to the Monin-Obukhov similarity theory, the surface layer profiles were in agreement [15]. In contrast, wind profiles were considered to be constants above the surface layer [6]. Numerical model results were obtained for several combinations of surface roughness ($z_0$=0.025, 0.25, and 2.5 m), surface heat flux ($H_0$=110, 0, -40 $wm^{-2}$), and upper level wind speed (5, 10, and 15 $ms^{-1}$) with a stated surface-layer height of 85 m and a mixing height of 275 m.

For a given set of climatic conditions, the maximum Ground Level Concentration (g. l. c.) does not deviate much from the Gaussian model's prediction. Variations in surface roughness have an impact on the ground-level concentrations that the numerical model predicts. The zone of height concentration moves closer to the source as surface roughness increases, and the maximum g. l. c. rises in a manner similar to that of rising heat flow. Only in neutral stability is the normalized concentration $\bar{C}\bar{u}/Q$ independent of wind speed; in both stable and unstable settings, $\bar{C}\bar{u}/Q$ exhibits a notable reliance on upper-level wind speed.

In an evolving daytime PBL, Kao and Yeh [16] employed a more complex computational model of wind flow and dispersion. The time-dependent mean flow and diffusion equations listed below were resolved by them:

$$\frac{\partial \bar{C}}{\partial t} + \bar{u}\frac{\partial \bar{C}}{\partial x} + \bar{v}\frac{\partial \bar{C}}{\partial y} = K_y\frac{\partial^2 \bar{C}}{\partial y^2} + \frac{\partial}{\partial z}\left(K_z\frac{\partial \bar{C}}{\partial z}\right) \quad (4)$$

$$\frac{\partial \bar{u}}{\partial t} - f(\bar{v} - v_g) = \frac{\partial}{\partial z}\left(K_m\frac{\partial \bar{u}}{\partial z}\right) \quad (5)$$

$$\frac{\partial \bar{v}}{\partial t} + f(\bar{u} - u_g) = \frac{\partial}{\partial z}\left(K_m\frac{\partial \bar{v}}{\partial z}\right) \quad (6)$$

$$\frac{\partial \bar{\theta}}{\partial t} = \frac{\partial}{\partial z}\left(K_h\frac{\partial \bar{\theta}}{\partial z}\right) \quad (7)$$

The planetary boundary layer's vertical eddy diffusivities of heat and momentum were specified as follows, whereas the surface layers were prescribed based on the Monin-Obukhov similarity relations [17]:

$$K_m = \lambda^2\left[\left(\frac{\partial \bar{u}}{\partial z}\right)^2 + \left(\frac{\partial \bar{v}}{\partial z}\right)^2 - \frac{g}{T_0}\frac{\partial \bar{\theta}}{\partial z}\frac{K_h}{K_m}\right]^{1/2} \quad (8)$$

where, the scale of eddies that contain energy is denoted by λ. The influence of stability is explicitly included in terms of the flux Richardson number in this mixing-length style of formulation for $K_m$:

$$K_m = \lambda^2\left|\frac{\partial \bar{v}}{\partial z}\right|(1 - Rf)^{1/2} \quad (9)$$

Using the surface layer similarity relations, ref. [18] calculated the ratio of eddy diffusivities $K_h/K_m$. Based on observations made during the Great Plains field program, they described them as functions of height and time for an average day, assuming $K_y=K_z=K_h$ throughout the PBL. In order to solve the above set of governing equations numerically, the initial temperature profile, constant geostrophic winds ($u_g$=10 ms$^{-1}$ and $v_g$=0), and the diurnally fluctuating surface heat flow were also supplied.

Given that the wind-direction and wind-speed shears in the central portion of the PBL both diminish as the inversion height rises with increasing time, the calculated mean velocity profiles seem to be realistic. The cross-isobar angle's vertical profiles indicate that it decreases with height and with the time of day. By mid-afternoon, the PBL has grown to a depth of 1100 meters, and wind-direction shears are sufficiently minor to be ignored. However, the gradient transport theory seems to have overstated the wind-speed and wind-direction shear in the model [2].

## 4.Turbulence Kinetic Energy Models

The mean advection-diffusion equation is solved for the given eddy diffusivities and mean transport winds in the most basic kind of gradient transport models. With a first-order closure scheme and a defined eddy viscosity or mixing length, mean winds are occasionally also calculated from the equations of mean motion [19]. Only in an idealized PBL can the exact specification of diffusivity or eddy viscosity be justified. It is necessary to relate eddy diffusivities to turbulence velocity and length scales and carry dynamical equations for the same in order to properly specify them. The Turbulence Kinetic Energy (TKE) equation is employed in the most popular method:

$$\frac{DE}{Dt} = -\left[\overline{\acute{u}\acute{w}}\frac{\partial \bar{u}}{\partial z} + \overline{\acute{v}\acute{w}}\frac{\partial \bar{v}}{\partial z}\right] + \frac{g}{T_w}\overline{\acute{w}\acute{\theta}_v} - \frac{\partial}{\partial z}\left(\overline{\acute{w}\acute{E}} + \frac{\overline{\acute{w}\acute{p}}}{P_9}\right) - \varepsilon \quad (10)$$

where E and É are the mean and fluctuating turbulence kinetic energies per unit mass.

$$E = \frac{1}{2}\left(\overline{\acute{u}^2} + \overline{\acute{v}^2} + \overline{\acute{w}^2}\right) \quad (11)$$

$$\acute{E} = \frac{1}{2}\left(\acute{u}^2 + \acute{v}^2 + \acute{w}^2\right) \quad (12)$$

The various terms on the right-hand side of Eq. (10) represent turbulent transport, shear production, buoyancy production or destruction, and the rate of dissipation of the TKE, while the left-hand side represents the total derivative, which includes both the rate of change with time and the advection by mean flow.

## 5.The Parameterized Length Scale Model

All of the right-hand-side terms in Eq. (10) are parameterized in simpler TKE models. The K-theory parameterizations of heat and momentum fluxes have already been covered. Similarly, the turbulent transport term is parameterized as follows:

$$\overline{\acute{w}\acute{E}} + \frac{\overline{\acute{w}\acute{p}}}{\rho_0} = -k_E\frac{\partial E}{\partial z} \quad (13)$$

Similar to the turbulent Prandtl number, which is defined in terms of a dissipation length scale as follows, the diffusivity of TKE is assumed to be equal to or proportional to Km, meaning that $K_E = K_m/\sigma_E$ where $\sigma_E$ is the diffusivity ratio.

$$\varepsilon = \frac{C_\varepsilon E^{3/2}}{\ell_\varepsilon} \quad (14)$$

where, the dissipation length $\ell_E$ is related to the large-eddy length scale $\ell$ in a similar way as the mixing length $\ell_m$, and $C_\varepsilon$ is an empirical constant. While some researchers have distinguished between these length scales, the majority of TKE models assume that $\ell_z = \ell_m = \ell$ [20]. The eddy viscosity is most frequently expressed as follows:

$$K_m = C\ell E^{1/2} \quad (15)$$

which, Prandtl and Kolmogorov [21] proposed. In this case, C is an empirical constant that might vary depending on how $\ell$ is defined. It is commonly thought that the vertical diffusivities of mass and heat are proportional to Km. The $K_h/K_m$ and $K_z/K_m$ ratios are occasionally interpreted as stability functions. Although eddy diffusivities are calculated using physically valid relationships involving stability and turbulence, the TKE closure is likewise predicated on the gradient transfer theory. Note that Eq. (15) implies that $K_m$ is proportional to both the large-eddy length scale ($\ell$)and the turbulence velocity scale$\left(E^{1/2}\right)$. For the latter, the prognostic equation is the TKE equation. In the literature, numerous prognostic and diagnostic expressions for l have been proposed [22]. While some of them only apply to the neutral PBL, others use stability effects in various formulas for $\ell$ and $\ell_\varepsilon$ [23].

## 6.The $E-\varepsilon$ Model

In more sophisticated, but not necessarily more accurate, TKE models an additional dynamical equation for the rate

of energy dissipation ε, or the large-eddy (mixing) Length scale $\ell$, is carried in the model. Using a prognostic equation for "ε or $\ell$" eliminates the need for parameterizing the same [24]. An equation for ε is more common because the concept of energy dissipation is easier to grasp than that of a mixing length. In terms of E and ε, eddy viscosity is usually expressed as:

$$K_m = \frac{C_k E^2}{\varepsilon} \tag{16}$$

where, $C_k$ is an empirical constant that may depend on the type of flow. The ε equation contains many new unknown terms that have to be considerably simplified and parameterized. The highly parameterized form used in the-called $E-\varepsilon$ or $k-\varepsilon$ models is given as:

$$\frac{D\varepsilon}{Dt} = C_1\frac{\varepsilon}{E}\left[-\overline{\acute{u}\acute{w}}\frac{\partial \bar{u}}{\partial z} - \overline{\acute{v}\acute{w}}\frac{\partial \bar{v}}{\partial z} + \frac{g}{T_{v0}}\overline{\acute{\theta}_v\acute{w}}\right] - C_2\frac{\varepsilon^2}{E} + \frac{\partial}{\partial z}\left(K_\varepsilon\frac{\partial \varepsilon}{\partial z}\right) \tag{17}$$

where $C_1$ and $C_2$ are empirical constants and $K_\varepsilon$ is the vertical diffusivity of dissipation, which is usually linked to that of momentum as $K_\varepsilon = K_m/\sigma_\varepsilon$ . Here, $\sigma_\varepsilon$ is the inverse of the diffusivity ratio, similar to the turbulent Prandtl number. The various terms on the right-hand side of Eq. (17) represent production, destruction, and turbulent transport of dissipation, respectively. The production and destruction terms in their parameterized forms have been assumed to be proportional to the production and dissipation of TKE. The various constants ($C_k$, $C_1$, $C_2$, etc.) in the so-called $E-\varepsilon$ or $k-\varepsilon$ model have been estimated from the laboratory experimental data. The "standard" values of the same may not be appropriate for the stratified, rotating atmospheric PBL [22-23]. Yet sufficiently accurate measurements of production, dissipation, and turbulent transport terms in the TKE and ε equations are not available for a direct empirical determination of these constants for the PBL. Different values have been suggested from comparisons of model-predicted and observed wind and eddy viscosity profiles by different investigators [23, 25].

## 7.The $E-\ell$ Model

In this model, the eddy viscosity is determined by Eq. (15) with E and $\ell$ computed from their dynamical equations. Thus, instead of the ε equation, a prognostic equation for the length scale $\ell$ (more appropriately, the product $E\ell$) is included in the model. Mellor and Yamada proposed such a model as a compromise between their level 2 and 3 models. The parameterized form of the prognostic equation for $E\ell$ looks similar to that for the dissipation rate ε [26]. It also has the same limitations of highly uncertain closure constants.

A comprehensive review of the different types of TKE-closure models has been given by ref. [27]. They also tested some of the models with different parameterization schemes against limited field experimental data. One of their two general conclusions is that mean profiles of potential temperature, humidity, and horizontal wind components show little sensitivity to the type of closure scheme as long as the effects of turbulent mixing in the PBL are properly handled. Thus, in the determination of $K_m$ using a diagnostic formulation of $\ell$ or a prognostic determination of ε makes little difference. The second main conclusion is that the TKE closure shows closer agreement with the observed turbulence structure in the PBL than the first-order closure. Among the diffusion TKE models as a group, the $E-\varepsilon$ model performs better than the parameterized ε model. This is because the former contains more physics of energy dissipation. Among $E-\varepsilon$ parameterizations, the modified [28] scheme performed best. It should be emphasized that these conclusions are based on rather limited comparisons of model results with one day's observations in a convective marine boundary layer. Here we consider only the first-order closure or gradient diffusion model. In this, the vertical diffusivity of material is often assumed equal to that of heat, which is assumed proportional to eddy viscosity, that is $K_z = K_h = \alpha K_m$, where α may be specified as a function of stability. The horizontal diffusivities must also be specified in order to solve the mean diffusion equation, these may be assumed proportional to $E^{1/2}$ and also proportional to the large-eddy length scale in the appropriate direction. Since information about the latter may not be available, horizontal diffusivities are usually assumed equal or proportional to the vertical diffusivity. Such as assumption appears to be reasonable for short-range dispersion, but becomes invalid for mesoscale and regional dispersion.

The TKE closure has a definite advantage over the simple gradient transport approach in that the eddy diffusivities are directly related to the turbulence kinetic energy and computed from the TKE equation. In the $E-\ell$ and $E-\varepsilon$ models, even the large-eddy length scale is computed rather than explicitly specified. Such models represent a reasonable compromise between the overly simplistic gradient transport models and much more complicated second and higher order closure models. They are particularly useful for modeling dispersion in non-homogeneous, flows over complex terrain and around buildings. Most of the conceptual limitations of the k-theory remain in the TKE-closure models as well.

## 8.Higher Order Closure Models

The second moment equations contain the unknown third moments correlations involving pressure and velocity or other scalar fluctuations, and the molecular dissipation terms, which have to be parameterized to close the set of equations, that is to reduce the number of unknowns to the number of equations. Thus, the closure problem shifts to the higher order second-momentum equations. The models based on the first-and second moment equations are called second-order closure models. Certainly, the second-moment equations contain considerable amounts of physical information regarding the dynamics of turbulent fluctuations. Therefore, it has been argued that the second-order closure approach should be more general than the

first-order closure. Similarity, a third-order closure model utilizing the dynamical equations for first, second, and third moments might be considered even more general because it contains more physics of turbulence [29].

## 9.Second-order Closure Methods: Parameterization of Turbulent Transport

The third moment terms appearing in the second-moment equations cause the fundamental closure problem of the latter. Physically, they represent the turbulent transports of second moments and are found to be rather insignificant in stably stratified flows including the SBL. The vertical turbulent transports have been observed to become very important and often govern the dynamics of unstable and convective boundary layers. Their accurate parameterization is considered crucial to the proper modeling of the CBL using the second-order closure approach. The simplest and the most commonly used parameterization of turbulent transport is based on the gradient-diffusion concept, whereby third moments are expressed as the products of second moments and some form of turbulent diffusivity. The diffusivity is expressed either as a product of turbulence length and velocity scales, as in Eq. (15), or in terms of the turbulence kinetic energy (E) and the rate of energy dissipation, as in Eq. (16) [30-31]. In the latter approach, a turbulence diffusion time scale is defined as $\tau_D = E/\varepsilon$ and the diffusivity is expressed as $K \sim \tau_D E$ which is consistent with Eq. (16).

Both of the third-moment parameterization methods are based on the concept of down-gradient diffusion. The same concept, when applied to second moments in the first-order and TKE closure models, has been found to be inconsistent with observations in the convective boundary layer. Measurements of third moments in the CBL indicate that the buoyancy-driven turbulence can also cause counter-gradient transport of second moments. However, the partial failure of the gradient transport hypothesis for third moments does not appear to be as catastrophic as that for second moments. For this reason, the second-order closure models using the simpler gradient transport hypothesis have simulated most of the mean flow and turbulence structure reasonably well. A more complicated functional expansion approach, originally proposed by ref. [32], can remove some of the limitations of the simple approach, but it also introduces many more terms and empirical constants whose values cannot be determined from the available experimental data. Another approach is to carry the dynamical equations for third moments, but these have their own closure problems [33-34].

### 9.1.Parameterization of dissipation

An accurate modeling or parameterization of the molecular dissipation terms in the second-moment equations, particularly the variance equations, is important because these terms determine the rate at which turbulence variances and kinetic energy are destroyed. In some models, $\varepsilon$ also determines the turbulence length and time scales that are used in the parameterization of turbulent transport and pressure terms. In the simplest approach $\varepsilon, \varepsilon_\theta$, and so on are expressed in terms of the appropriate length and velocity scales (14). Alternatively, dynamical equations are also carried for $\varepsilon, \varepsilon_\theta$, etcetera. Such equations are very complex [35] and only highly simplified and parameterized forms of the same, such as Eq. (17), are used in second-order closure models [30-31]. The molecular dissipation terms in the dynamical equations for covariance's or fluxes are usually neglected, using Kolmogorov's local-isotropy hypothesis for large Reynolds number flows. The same hypothesis also implies that the rate of dissipation is the same for the energies associated with different velocity components, that is, $\varepsilon_u = \varepsilon_v = \varepsilon_w = \varepsilon/3$.

### 9.2.Parameterization of Return-to-Isotropy Terms

The parameterization of the covariance's between fluctuating pressure and fluctuating velocity, temperature, or other scales gradients is probably the most difficult problem of higher order closure modeling. These pressure terms are also called the return-to-isotropy terms because they tend to equalize the different velocity variances through redistribution of energy between them and act to destroy any covariance's of energy between them and act to destroy any covariance's in the flow. These are the primary destruction terms in the covariance equations, since molecular dissipation terms become negligibly small due to local isotropy. For this reason, the simplest way to parameterize these terms is to make them proportional to the excess variance or covariance to be destroyed and inversely proportional to the time scale of turbulence [36]. Thus, the return-to-isotropy term in the dynamical equation for the covariance $\overline{\acute{c}\acute{u}}$ can simply be parameterized by $-\overline{\acute{c}\acute{u}}/\tau_D$ multiplied by an empirical constant. This simplistic approach has not been found to be entirely satisfactory and more complex parameterizations have been proposed [32-33].

The model of ref. [37] was slightly modified by ref. [38] to permit some counter gradient heat flux as:

$$\overline{\acute{w}\acute{\theta}} = -K_h\left(\frac{\partial\bar{\theta}}{\partial z} - \nu_c\right) \tag{18}$$

This modification to the original gradient transport relationship, with $\nu_c = 0.5\text{x}10^{-3}$ $\text{Km}^{-1}$, resulted in a better agreement with the observed concentrations. In particular, the model-computed ground-level concentrations due to surface and elevated sources agree well with observations as well as with other more sophisticated numerical simulations. Other plume statistics such as the mean plume height and the standard deviation of the vertical concentration distribution also agree with measurements.

For the more general filter operations that may not preserve previously filtered average variables on a second-filter operation or averaging, that is, for which $\bar{\bar{u}} = \bar{u}$ and so on, additional terms are generated by the averaging or filter operation on the instantaneous equations. For these, each of

the subgrid-scale Reynolds fluxes inside the parentheses on the right-hand sides is replaced by two terms, for example:

$$\overline{\acute{u}^2} \rightarrow \overline{u^2} - \bar{u}^2$$

$$\overline{\acute{u}\acute{v}} \rightarrow \overline{uv} - \bar{u}\bar{v}$$

$$\overline{\acute{u}\acute{w}} \rightarrow \overline{uw} - \bar{u}\bar{w} \quad (19)$$

where → denotes that the left-hand term is to be replaced by the right-hand terms, but the two are not necessarily equal using the Cartesian tensor notation for velocity $u_i$ with i=1,2 and 3 representing the three components, one can write, in general:

$$\overline{\acute{u}_i\acute{u}_j} \rightarrow \overline{u_iu_j} - \bar{u}_i\bar{u}_j \quad (20)$$

By substituting $u_i = \bar{u}_i + \acute{u}_i$ and $u_j = \bar{u}_j + \acute{u}_j$ , and taking the average, it is easy to show that the two sides of arrow in Eq. (20) are different as:

$$\overline{\acute{u}_i\acute{u}_j} = \overline{\bar{u}_i\bar{u}_j} + \overline{\acute{u}_i\bar{u}_j} + \overline{\bar{u}_i\acute{u}_j} + \overline{\acute{u}_i\acute{u}_j} \quad (21)$$

Only for the particular filters satisfying the conditions $\bar{\bar{u}} = \bar{u}$, etc. the two sides of Eq. (20) become exactly equal. Even otherwise the RHS is often considered as a combined subgrid-scale Reynolds stress tensor $\tau_{ij}$ i.e.

$$\tau_{ij} = \overline{u_iu_j} - \bar{u}_i\bar{u}_j \quad (22)$$

For the sake of convenience between the grid volume-averaged or filtered equations used in LES are often written in the same form as the ensemble averaged equations, implying a strong correspondence between $\tau_{ij}$ and $\overline{\acute{u}_i\acute{u}_j}$.

## 10.Subgrid-scale models

In order to close the set of grid-volume averaged or filtered equations, the unknown SGS Reynolds stresses and fluxes must be parameterized in terms of the resolved variables for which the set LES equations is numerically solved. The values SGS-closure approaches or models have been reviewed among others by [39].

### 10.1.Lagrangian Stochastic Models

In the Lagrangian approach to dispersion modeling, one tracks particles through a turbulent environment using either a numerically computed Eulerian velocity field or a stochastic model for the Lagrangian particles velocities [40]. Followed the former approach using the velocity field calculated in large-eddy simulation of the CBL. The successful applications of this approach to atmospheric dispersion have already been discussed in the preceding section [41]. The Lagrangian particle-dispersion modeling utilizing the LES for mean flow and turbulent velocity fields is the most computer intensive and expensive approach. The instantaneous velocities at all the grid points at each time step must be stored in the computer memory for calculation of the trajectories of thousands of particles, and hence, obtaining of the desired dispersion statistics.

The second approach is much less expensive and is based on a stochastic model of the Lagrangian particle velocity. The model first separates the instantaneous velocity into a mean and a turbulent component [42] that is:

$$\frac{dX_i}{dt} = U_i = \bar{U}_i + \acute{U}_i \quad (23)$$

In which the overbar represents time averaging and prime, as usual denotes turbulent fluctuation by definition the Lagrangian velocity $U_i$ corresponds to an individual particle.

### 10.2.Random-walk Model for Homogeneous turbulence

Smith [43] proposed a random-walk hypothesis that states that the Lagrangian turbulent velocity a short time later can be expressed in terms of its previous velocity and a random velocity fluctuation, that is:

$$\acute{U}_i(t + \Delta t) = R_L(\Delta t)\acute{U}_i(t) + \acute{\acute{U}}_i \quad (24)$$

Here, $R_L(\Delta t)$ is the value of the Lagrangian autocorrelation function $R_L(\xi)$ $at\ \xi = \Delta t$ and $\acute{\acute{U}}_i$ is the purely random or the uncorrelated part of velocity fluctuation. Smith [44] called Eq. (45) a linear regression equation, because he could fit a straight line through a plot of experimentally measured values of $\acute{V}(t + \Delta t)$ versus $\acute{V}(t)$ [45]. To specify the Lagrangian particle velocity at each time step in the numerical model using Eq. (24), one must specify $R_L(\Delta t)$ as well as $\acute{\acute{U}}_i(t)$. The former is easily obtained from the commonly used exponential form of the Lagrangian autocorrelation function, that is:

$$R_L(\Delta t) = exp\left(-\frac{\Delta t}{T_{iL}}\right) \quad (25)$$

Provided the integral time scale can be specified. The random fluctuation $\acute{\acute{U}}_i$ is picked from a very large ensemble of random numbers whose mean is zero and the variance is given by:

$$\bar{\acute{\acute{U}}}_i^2 = \overline{\acute{U}_i^2}[1 - R_L^2(\Delta t)] \quad (26)$$

where, the repeated index does not imply summation. Eq. (47) is obtained by squaring and averaging Eq. (24) and assuming that the velocity variance does not change during the short time interval$\Delta t$. It is more convenient to express $\acute{\acute{U}}_i$ in terms of its standard deviation, that is;

$$\acute{\acute{U}}_i = \sigma_i[1 - R_L^2(\Delta t)]^{1/2}\eta(t) \quad (27)$$

where, $\sigma_i$ is the standard deviation of the velocity fluctuations $\acute{U}_i$ and $\eta(t)$ is a dimensionless random variable with zero mean and variance=1. Substituting from Eqns. (25) and (27) into Eq. (24), one obtains:

$$\acute{U}_i(t + \Delta t) = a\acute{U}_i(t) + \sigma_i(1 - a^2)^{1/2}\eta(t) \quad (28)$$

where,

$$a = exp\left(-\frac{\Delta t}{T_{iL}}\right) \quad (29)$$

or some other suitable expression or value for $R_L(\Delta t)$. For

very large time steps with $\Delta t >> T_{iL}$, $a \cong 0$, so that the velocity at any time is completely specified by $\sigma_i \eta(t)$ and is not correlated at all with its value at the previous time. The Langevin equation is related to Markov-chain models of Lagrangian velocityby [46]. They start with the one-dimensional equation for the vertical particle velocity:

$$\frac{dW}{dt} = -\alpha W + \lambda \xi(t) \quad (30)$$

where, $\alpha$ and $\lambda$ are coefficients to be specified later and $\xi(t)$ is Gaussian white noise, which is a stationary stochastic process with a Gaussian probability density function and zero mean. The solution to the above stochastic differential equation is given by:

$$W(t) = W(0)e^{-\alpha t} + \lambda \int_0^t e^{\alpha(x-t)}\, \xi(s) ds \quad (31)$$

which, is then decomposed into mean and fluctuating parts as follows:

$$\bar{W}(t) = \bar{W}(0)e^{-\alpha t} \quad (32)$$

$$\acute{W}(t) = \acute{W}(0)e^{-\alpha t} + \lambda \int_0^t e^{\alpha(s-t)}\, \xi(s) ds \quad (33)$$

From Eq. (33), the following expressions for the variance and covariance of vertical velocity are derived by [47] as follows:

$$\overline{\acute{W}^2}(t) = \overline{\acute{W}^2}(0)e^{-2\alpha t} + \frac{\lambda^2}{2\alpha}(1 - e^{-2\alpha t}) \quad (34)$$

$$\overline{\acute{W}(0)\acute{W}(t)} = \overline{\acute{W}^2}(0)e^{-\alpha t} \quad (35)$$

If the Lagrangian integral time scales for the particle velocity is defined as:

$$T_{iL} = \int_0^\infty \frac{\overline{\acute{W}(0)\acute{W}(t)} dt}{\overline{\acute{W}^2}(0)} \quad (36)$$

Eqns. (34) and (35) for the variance and covariance enable the coefficient in the langevin equation (30) to be determined as:

$$\alpha = \frac{1}{T_{iL}} \quad (37)$$

$$\lambda = \sigma_w \sqrt{2\alpha} = \sigma_w \left(\frac{2}{T_{iL}}\right)^{1/2} \quad (38)$$

Thus, if $\sigma_w$ and $T_{iL}$ are known. Eq. (30) determines the velocities, and therefore trajectories, of an ensemble of tagged fluid particles with a prescribed distribution of initial velocity W(0).

### 10.3.Random-walk Models for Inhomogeneous Turbulence

Dispersion in the lower part of the atmospheric boundary layer with $\sigma_w$ increasing with height, as happens in a canopy layer and also in the CBL is simulated by [46-47]. They found that the use of Eq. (27) resulted in far too may particles collecting in the near-surface region of low turbulence. They reasoned that, for $\partial\sigma_w / \partial z \geq 0$, the particles crossing an x-y plane going downward would have higher velocity on the average than those traveling upward. To satisfy the mass continuity across the x-y plane, the vertical Lagrangian velocity distribution must be skewed with a preference for upward motion. Therefore, a bias velocity is added to the Markov equation for the Lagrangian vertical velocity by [48]:

$$W(t + \Delta t) = aW(t) + \sigma_w(1 - a^2)^{1/2}\eta(t) + \Lambda_L \frac{\partial \sigma_w}{\partial z} \quad (39)$$

Here $\Lambda_L$ is a length scale whose values were found by comparing the model-predicted mean concentrations with those measured during the project Prairie Grass field experiment [49]. It is found that $\Lambda_L$ is function of height above the ground and stability. It should be noted that the vertical Lagrangian velocity W in Eq. (31) includes both the mean and fluctuating parts. The last term amounts to a positive bias to only the mean vertical velocity. It is assumed to be a function of height and stability, but independent of travel time. Hence, the appropriate Langevin equation for this case of inhomogeneous turbulence is:

$$\frac{dW}{dt} = -\alpha W + \lambda \xi(t) + F \quad (40)$$

where,

$$F = -\frac{1}{\rho_0}\frac{\partial \bar{P}_1}{\partial z} = \frac{\partial \overline{\acute{w}^2}}{\partial z} \quad (41)$$

Here $\bar{P}_1$ denotes the deviation of the mean pressure from the reference hydrostatic pressure $P_0$ and $\rho_0$ is the density of the reference atmosphere. Following an analysis of the Langevin equation similar to that for the case of stationary and homogeneous turbulence. But with some additional implied assumptions. An expression for the mean drift velocity is derived by [50]:

$$\bar{W}(t) = T_{iL}\frac{\partial \sigma_w^2}{\partial z} \quad (42)$$

The assumptions of stationary turbulence and $\overline{\acute{W}^2} = \overline{\acute{w}^2} = \sigma_w^2$ implied in the derivation of Eq. (42) are somewhat questionable in the case of non-homogeneous turbulence. However, the above result is consistent with the following, more general expression of the mean drift velocity of particles obtained form of diffusion equation:

$$\bar{W}(t) = T_{iL}\frac{\partial \sigma_w^2}{\partial z} + \sigma_w^2 \frac{\partial T_{iL}}{\partial z} \quad (43)$$

Since the questionable assumption of $T_{iL}$=constant, implied by constantα, was made in the derivation of Eq. (42), the use of Eq. (43) should be preferable. With the addition of mean drift velocity, the appropriate Markov-chain equation for the vertical particle velocity is:

$$W(t + \Delta t) = aW(t) + \sigma_w(1 - a^2)^{1/2}\eta(t) + T_{iL}\frac{\partial \sigma_w^2}{\partial z} + \sigma_w^2 \frac{\partial T_{iL}}{\partial z} \quad (44)$$

A more general form of the nonlinear stochastic differential equation for the vertical velocity has been used in more recent random-walk models of dispersion [48-51]:

$$dW = A(Z,W)dt + B(Z,W)d\eta \quad (45)$$

Here A and B are functions of particle position (Z) and vertical velocity (W), and dη is the random velocity increment. For the more general vector or tensor form of the stochastic differential equation, one should refer to [49, 52]. In high Reynolds number flows the evolution of the particle velocity W(t) can be assumed to be a Markov process because the particle acceleration is significantly correlated only for times much shorter than the lifetime of the energetic eddies. Hence the derivative dW can be represented by a nonlinear stochastic equation of the form (45). If P(Z, W) is the joint probability density function of all tracer or marked fluid particles in the ensemble of flows, then away from any source it should satisfy the Fokker-Planck equation [49, 52]:

$$W\frac{\partial P}{\partial Z} + \frac{\partial (AP)}{\partial W} = \frac{\partial^2 (B^2 P)}{2\,\partial W^2} \quad (46)$$

For the simplest problem of one-particle dispersion in stationary and homogeneous turbulence, $A = -W/T_{iL}$ and $B = \sqrt{2}\,\sigma_w/T_{iL}^{1/2} = (c_0\varepsilon)^{1/2}$, where $c_0 = 2.0$ is Kolmogorov's structure function constant and ε is the rate of energy dissipation. For certain inhomogeneous turbulent flows, such as the surface layer and CBL, A and B have been determined uniquely for the one-dimensional case [44-45]. For the more general three-dimensional dispersion problems, however, the solutions to Eq. (46) may not be unique [52]. Wilson and Sawford [48] have reviewed the theoretical basis for and the advantage of the Lagrangian stochastic or random-walk models for dispersion in the PBL.

## 11.Computation of particle Trajectories and Mean Concentrations

Fluctuating velocities are computed at each time step using the random-walk models or Markhov-chain expressions [53] discussed in the preceding subsection. For example, the vertical displacement of the particle is given by:

$$dZ = W(t)dt \quad (47)$$

or

$$Z(t+1) = Z(t) + W(t)\Delta t \quad (48)$$

in which $\Delta t$ is chosen as a small fraction (10-20%) of $T_{iL}$. The vertical inhomogeneity of the PBL turbulence requires small time steps in random-walk models of particle dispersion.

In practice, particle displacement is calculated for short time increments $(\Delta t)$ and number of increments $(n_j)$ that all particles spend in a particular grid cell or volume $\Delta x\Delta y\Delta z$.. If the continuous point source strength is Q and the total number of trajectories is N, then the mean concentration in the grid cell j is [54-55]:

$$C_j = \frac{n_j \Delta t Q}{N\Delta x\Delta y\Delta z} \quad (49)$$

This method gives a minimum definable concentration for $n_j = 1$ and also a maximum definable concentration corresponding to $n_j = N\Delta x/\bar{u}\Delta t$. It is necessary to make a suitable choice of model parameters to ensure that the concentration range of interest is covered. Since the ratio of the maximum to the minimum definable concentration is $N\Delta x/\bar{u}\Delta t$, to obtain a wide range of concentration estimates large numbers of trajectories must be computed with small time steps relative to the time taken to advect a particle through a cell Both of these require large compute time. In practice the grid cells are allowed to expand in size with increasing downwind distance, so that decreasing concentrations may be resolved.

An alternative method of computing mean particle concentrations is based on the expression:

$$\bar{C}(x,t) = Q\int_{-\infty}^{t} \rho(x_i, t, \acute{x}_i, \acute{t})\, d\acute{t} \quad (50)$$

where, $\rho$ is the probability density that a particle released at $\acute{x}_i$ at time $\acute{t}$ will be found at $x_i$ at time t. The probability density function can be estimated from a large ensemble of particle trajectories [41].

## 12.Dispersion in the Surface Layer

Two-dimensional dispersion in the neutral surface layer is modeled using the Markov-chain equation (28) for the vertical velocity fluctuation by [54]. He assumed that $\bar{W} = 0$, $\bar{U}(z)$ is given by the log law, and $U(t) = \bar{U}(z) \pm \sigma_u$, in which the plus or minus sign was determined by a probability density such that $\acute{U}\acute{W}/\sigma_u\sigma_w = -0.25$. Using the neutral surface-layer similarity relations, the following parameters are specified $\sigma_u = 2.2u_*$, $\sigma_w = 1.3u_*$, and $T_{iL} = 2.4z/\bar{u}$ by [56]. His random-walk simulations of dispersion in the neutral surface layer showed good agreement with field experimental data.

The same formulations for the vertical velocity are used by [54] as Hall's, but ignored longitudinal velocity fluctuations. He estimated $T_{iL} = 0.26z/u_*$ using the alternative expressions for eddy diffusivity $K = \sigma_w^2 T_{iL} = kzu_*$ in the neutral surface layer in conjunction with $\sigma_w^2 \approx 1.56u_*^2$. Another theoretical approach based on an empirical form of the spectrum of vertical velocity yielded $T_{iL} \approx 0.60z/u_*$ , but the best agreement with field experimental data was obtained with $T_{iL} = 0.4z/u_*$. Two-dimensional random-walk simulations of dispersion in the neutral surface layer were made for surface and elevated releases.

### 12.1.Dispersion in the Neutral PBL

The formulation of random-walk modeling is extended to simulate dispersion from elevated source in the whole PBL under near-neutral conditions by [57]. He used a Markov-chain expression for the vertical velocity very similar to Eq. (44), but with the difference that the last term representing drifts velocity was reduced by a factor $(1-a)$. For the longitudinal velocity fluctuation $\acute{U}$, a modified Markov

relation accounting for the desired correlation between $\acute{U}$ and $\acute{W}$ was utilized, although longitudinal velocity fluctuations were found to have a relatively small effect on model predictions. The mean wind and stress profiles in the neutral PBL were specified using an obscure analytical model, while turbulence parameters $\sigma_u, \sigma_w, T_{lu}, T_{Lw}$ were specified on the basis of empirical data on PBL turbulence.

Following the demonstrated good agreement with empirical dispersion curves, systematically the effects of H, $z_0$, and $u_*$ on the mean plume height($\bar{z}$) were investigated by [57], the $\sigma_z$, and the normalized g. l. c. It is found that, at al downwind distances, $\sigma_z$ decreases slightly with an increase in release height. For a fixed H and $z_0$, an increase in $u_*$ results in larger values of $\bar{z}$ and $\sigma_z$. The strong sensitivity of $\sigma_z$ to $u_*$ or $\bar{u}$ has not been considered in widely used empirical dispersion curves or formulas.

### 12.2.Dispersion in the CBL

Measurements and large eddy simulations of vertical velocity fluctuations in the convective boundary layer (CBL) have revealed that the corresponding PDF is positively skewed, but has a negative mode. This of course, is a consequence of the organized convective circulation in the CBL, characterized by updrafts and downdrafts [2]. LES model demonstrated the surprising effects of a skewed PDF of vertical velocity on dispersion from surface and elevated sources in the CBL. For a surface source, the maximum concentration in the plume stayed at the ground level only for a relatively short dimensionless travel time or distance X, from the source and then it lifted off the ground and slowly moved to the upper part of the CBL. On the other hand, the height of maximum concentration due to an elevated source decreased with downwind distance, touched the surface and then lifted off. This has been attributed to larger areas of slower moving downdrafts and smaller areas of faster moving updrafts, that is, to the skewness of the vertical distribution

### 12.3.Dispersion in the stable Boundary Layer and Katabatic Flows

Compared with their use for the neutral and convective boundary layers, random walk models, along with other aspects of turbulence and dispersion, are not so well developed for the stable boundary layer (SBL). Three different formulations of dispersion are developed and tested in stably stratified katabatic flows in which turbulence was assumed to be inhomogeneous with a Gaussian PDF by [58]. The parameters influencing dispersion in a katabatic flow are the layer thickness, mean velocities, and turbulence, all of which vary with downwind distance. They used the two-dimensional katabatic flow model of ref. [59], which is based on the TKE closure. Their simplest random walk formulation assumed that particle velocities are not correlated at all over the duration of time step. This leads to a pure random-walk model in which the increment in particle height Z(t) is expressed in terms of the time step, the height-dependent vertical-eddy diffusivity, the mean Eulerian vertical velocity, and random forcing function. Another more accurate and also more complex formulation is based on the Langevin equation and is similar to that proposed by [49].

### 12.4.Dispersion in Mesoscale and Complex Terrain Flows

Random-walk Lagrangian transport and dispersion models have been combined with mesoscale atmospheric models to simulate dispersion in mesoscale and complex terrain flows [39, 60-71]. These models are typically applied over domain sizes of 50 to 500 km, with a horizontal resolution of 1 to 10 km. Particle velocity consists of two components: (1) the resolved mean velocity from the mesoscale model and (2) the turbulent fluctuating velocity from the Lagrangian stochastic model. The mesoscale model provides the various parameters needed in the dispersion model, such as the mixing height, the surface fluxes of momentum, and heat, and in some cases the turbulence kinetic energy. From these, turbulence variables ( $\sigma_W, \sigma_X, \sigma_W, T_L, etc.$) are estimated from diagnostic relations based on empirical similarity relations. The widespread use of diagnostic similarity relations developed from similarity theories and experimental data for the horizontally homogeneous atmospheric boundary layer in complex terrain floes is a questionable practice.

### 13. Gaussian Turbulence

A Gaussian method is applied in equation

$$a_i(x_i, u_i) = \frac{1}{p}\left[\frac{\partial}{\partial u_i}\left(\frac{b_i^2 p}{2}\right) + \phi_i(x_i, u_i)\right]$$

At the initial value problem

$$\frac{dy}{dt} = f(y,t), \;\; y(t_0) = y_0 \qquad \text{(A)}$$

$f(y,t)$ is a continous function. One use Picard's iteration method [72] or the Method of Successive Approximations. It consists of constructing a sequence of functions $y^n(t)$ from the integral equation

$$y(t) = y_0 + \int_0^t f(y(\acute{t}), \acute{t})d\acute{t} \qquad \text{(B)}$$

To get the deterministic coefficient of the three-dimensional Langevin equation

$$a_i = -\left(\frac{C_0\varepsilon}{2\sigma_i^2}\right)u_i + \frac{1\partial\sigma_i^2}{2\partial x_j} + \frac{1}{2\sigma_i^2}\left(\frac{\sigma_i^2}{\partial x_j}\right)u_i^2 \qquad (51)$$

$$\frac{du_i}{dt} + \left(\frac{C_0\varepsilon}{2\sigma_i^2}\right)u_i = \frac{1\partial\sigma_i^2}{2\partial x_j} + \frac{1}{2\sigma_i^2}\left(\frac{\sigma_i^2}{\partial x_j}\right)u_i^2 + (C_0\varepsilon)^{1/2}\xi_i(t) \qquad (52)$$

$c_0 = 2.0$ is Kolmogorov's structure function constant and $\varepsilon$ is the rate of energy dissipation

$$\frac{\mathrm{du_i}}{\mathrm{dt}} + \alpha_i u_i = \beta_i + \gamma_i u_i^2 + (C_0\varepsilon)^{1/2}\xi_i(t) \qquad (53)$$

$$\alpha_i = \frac{C_0\varepsilon}{2\sigma_i^2}, \;\; \beta_i = \frac{1\partial\sigma_i^2}{2\partial x_j} \;\; \text{and} \;\; \gamma_i = \frac{1}{2\sigma_i^2}\left(\frac{\sigma_i^2}{\partial x_j}\right),$$

One determines exp $(\alpha_i t)$ as the integrating factor for the

equation (54). Multiplying the integrating factor by all terms in equation (53),

$$\frac{d[exp(\alpha_i t)u_i]}{dt} = \beta_i exp(\alpha_i t) + \gamma_i u_i^2 exp(\alpha_i t) + (C_0\varepsilon)^{1/2}\xi_i(t)exp(\alpha_i t) \quad (54)$$

$$u_i = (e^{-\alpha_i t}) \int_{t_0}^{t} [\beta_i \exp(\alpha_i \acute{t}) + \gamma_i u_i^2 \exp(\alpha_i \acute{t}) \left((C_0\varepsilon)^{1/2}\xi_i(\acute{t})\exp(\alpha_i \acute{t})\right] d\acute{t}) \quad (55)$$

Let

$$u_i^0 = \exp(-\alpha_i t) \int_{t_0}^{t} \left((C_0\varepsilon)^{1/2}\xi_i(\acute{t})\exp(\alpha_i \acute{t})\right] d\acute{t} \quad (56a)$$

The general iterative step is

$$u_i^{n+1} = exp(-\alpha_i t)[[u_i^0 + \int_{t_0}^{t} \exp(\alpha_i \acute{t}))(\beta_i + \gamma_i (u_i^2)^n + \left((C_0\varepsilon)^{1/2}\xi_i(\acute{t})\exp(\alpha_i \acute{t})\right] d\acute{t}] \times (u_i^n \rightarrow u_i^0) \quad (56b)$$

## 14. Results and discussion

The Iterative Langevin solution (ILS) approach is evaluated using the ground-level concentration data measured during the Copenhagen tracer experiment [73]. The Copenhagen experiment was carried out in the northern part of Copenhagen. The tracer (SF6) was released without buoyancy from a tower at a height of 115 m and collected at the ground-level positions in up to three crosswind arcs of tracer sampling units. The sampling units were positioned 2–6 km from the point of release. A total of nine tracer experiments were performed in stability conditions that are the result of the relative combination between neutral and convective (Table I). The site was mainly residential with a roughness length of 0.6 m. Wind speeds at 10 and 115 m are used to calculate the coefficient for the exponential wind vertical profile, which is used to obtain the wind speed as follows:

$$\gamma = [\frac{\log(u(115)}{\log(\frac{115}{10})}] \quad (57)$$

where, u (10) is the wind speed in 10 m and u (115) is the wind speed in 115 m

$$u(z) = u(10)\left[\frac{z}{10}\right]^{\nu} \quad (58)$$

**Table 1:** Meteorological parameters measured during the Copenhagen experiment

| Exp | u(ms$^{1}$) | $u_*$(ms$^{-1}$) | L (m) | $w_*$(ms$^{-1}$) | h(m) |
|---|---|---|---|---|---|
| 1 | 3.4 | 0.36 | -37 | 1.8 | 1980 |
| 2 | 10.6 | 0.73 | -292 | 1.8 | 1920 |
| 3 | 5.0 | 0.38 | -71 | 1.3 | 1120 |
| 4 | 4.6 | 0.38 | -131 | 0.7 | 390 |
| 5 | 6.7 | 0.45 | -444 | 0.7 | 820 |
| 6 | 13.2 | 1.05 | -432 | 2.0 | 1300 |
| 7 | 7.6 | 0.64 | -104 | 2.2 | 1850 |
| 8 | 9.4 | 0.69 | -56 | 2.2 | 810 |
| 9 | 10.5 | 0.75 | -289 | 1.9 | 2090 |

U wind speed (m/s), $u_*$ the friction velocity (m/s), L Monin Obukhov length(m), $W_*$ the convective vertical velocity (m/s) and h mixing height.

In this section we present the numerical simulations and comparisons with measured data of the Copenhagen experiment. Moreover, the results obtained with the ILS approach Eq. (44) are compared and a Gaussian model [72] and [73] using Eq. (56b) as in Table (2).

**Table 2:** Observed ground-level cross-wind-integrated concentration ($C_y$) and simulated by the ILS approach, and Gaussian model

| Run | Downwind distance (m) | Observed (μg/m$^2$) | Predicted concentration of $C_y$ (μg/m$^2$) | |
|---|---|---|---|---|
| | | | ILS Gaussian | Gaussian |
| 1 | 1900 | 2074 | 2550 | 2022 |
| 1 | 3700 | 739 | 715 | 1312 |
| 2 | 2100 | 1722 | 1670 | 1187 |
| 2 | 4200 | 944 | 1355 | 825 |
| 3 | 1900 | 2624 | 2699 | 2410 |
| 3 | 3700 | 1990 | 2050 | 1728 |
| 3 | 5400 | 1376 | 1562 | 1393 |
| 4 | 4000 | 2682 | 2850 | 1989 |
| 5 | 2100 | 2150 | 2235 | 1965 |
| 5 | 4200 | 1869 | 2355 | 1802 |
| 5 | 6100 | 1590 | 2100 | 1530 |
| 6 | 2000 | 1228 | 855 | 989 |
| 6 | 4200 | 688 | 730 | 741 |
| 6 | 5900 | 567 | 730 | 611 |
| 7 | 2000 | 1608 | 1650 | 984 |
| 7 | 4100 | 780 | 950 | 629 |
| 7 | 5300 | 535 | 833 | 533 |
| 8 | 1900 | 1248 | 1320 | 1263 |
| 8 | 3600 | 606 | 575 | 960 |
| 9 | 2100 | 1511 | 1720 | 1188 |
| 9 | 4200 | 1026 | 1250 | 805 |
| 9 | 6000 | 855 | 880 | 637 |

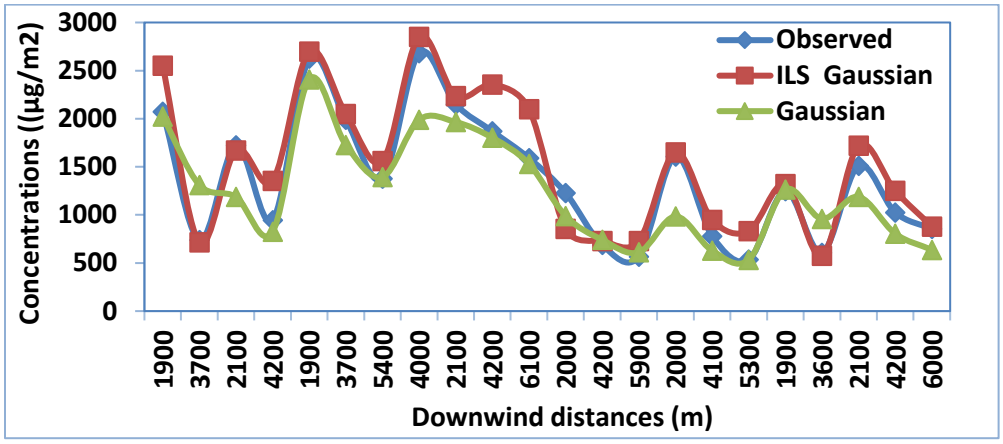


**Fig. 1:** Variation of the concentrations with downwind distance.

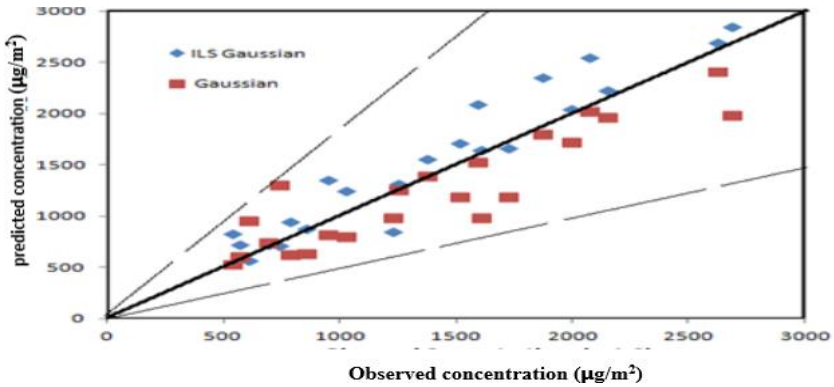


**Fig. 2:** Variations of predicted and Gaussian plume models with the observed

Additionally, Fig. (1) demonstrates that the predicted ILS and Gaussian iterative Langevin equation agree well and are closer observed concentrations Additionally, as Fig. (2) illustrates, the concentrations of the predicted ILS and Gaussian iterative Langevin equation are within a factor of two of the observed data.

## 15. Evaluation Statistics

For testing model accuracy, a statistical method is presented and comparison between predicted and observed results as offered by [74]. The following standard statistical performance measures that characterize the agreement between prediction ($C_p = C_{pred}/Q$) and observations ($C_O = C_{Obs}/Q$):

Fraction Bias (FB) $= \frac{(\overline{C_o} - \overline{C_p})}{[0.5(\overline{C_o} + \overline{C_p})]}$

Normalized Mean Square Error (NMSE) $= \frac{\overline{(C_p - C_o)^2}}{(\overline{C_p C_o})}$

Correlation Coefficient (COR) $= \frac{1}{N_m}\sum_{i=1}^{N_m}(C_{pi} - \overline{C_p}) \times \frac{(C_{oi} - \overline{C_o})}{(\sigma_p \sigma_o)}$

Factor of Two (FAC2) $= 0.5 \leq \frac{C_p}{C_o} \leq 2.0$

where $\sigma_p$ and $\sigma_o$ are the standard deviations of predicted $C_p$ and observed $C_o$ concentration respectively. Over bars refer to the average over all measurements. A perfect model must have the following performance: NMSE = FB = 0 and COR= FAC2 = 1.0. From the statistical evaluations, one finds that the two models are inside a factor of two with observed data; also, NMSE, FB, and the correlation coefficient are in good agreement with the observed data. Also ILS predicted and Gaussian model achieved 100% and 95% respectively.

**Table 3:** Statistical evaluation of predicted model in unstable condition.

| Model | NMSE | FB | COR | FAC2 |
|---|---|---|---|---|
| ILS Predicted | 0.03 | -0. 1 | 0.96 | 1.12 |
| Gaussian Predicted | 0.05 | 0.1 | 0.90 | 0.95 |

## 16. Conclusions

The predicted ILS and Gaussian iterative Langevin equation agree well and are closer observed concentrations additionally, as Fig. (2) illustrates, the concentrations of the predicted ILS and Gaussian iterative Langevin equation are within a factor of two of the observed data. From the statistical evaluations and stochastically analysis between the observed and predicted data, one finds that the two models are inside a factor of two with observed data, and also, NMSE, FB, and the correlation coefficient are in good agreement with the observed data. Also ILS predicted and

Gaussian model achieved 100% and 95% respectively.

**Statements and Declarations:**

No funds, grants, or other support was received

**Financial interests:** The authors declare they have no financial interests

**The data availability**

The authors declare that the data supporting the findings of this study are available within the paper and it was measured during the Copenhagen tracer experiment [71]. The Copenhagen experiment was carried out in the northern part of Copenhagen.

**Author Contribution declaration in the manuscript.**

Khaled Essa thought about the research, worked on creating the research, and wrote the research.

Ahmed Metwally wrote the research and made the drawings.

Fawzia Mubarak contributed to writing the research, creating graphics and statistics, and coordinating the research.

**Consent to publish declaration**

The authors agree well to publish this paper in journal of Ecology of Health and Environment

Ethics and Consent to Participate declarations

The authors agree on ethics and consent to participate declarations.

Please provide a Funding declaration. If there are no Funding, please state so.

Please my institute doesn't pay any money for publication (No funds)

**References**

[1] Jheyson Mejia Estrada: "Numerical simulation of atmospheric dispersion : application for interpretation and data assimilation of pollution optical measurements", 2022, https://theses.hal.science/tel-03739279v1.

[2] Fedorovich E.: "Dispersion of passive tracer in the atmospheric convective boundary layer with wind shears: a review of laboratory and numerical model studies", School of Meteorology, University of Oklahoma, Norman, USA, 2004.

[3] Davide Marucci, Matteo Carpentieri: "Dispersion in an array of buildings in stable and convective atmospheric conditions|", Atmospheric Environment, Volume 222, 2020, 117100

[4] Roberti D.R. ; R.P. Souto; H.F. de Campos Velho; G.A. Degrazia; D. Anfossi: "Parallel implementation of a Lagrangian stochastic model for pollution dispersion", in: 16th Symposium on Computer Architecture and High Performance Computing, 2004, Foz do Iguacu, Brazil, DOI: 10.1109/SBAC-PAD.2004.30

[5] Van Kampen N.G.: "Stochastic Processes in Physics and Chemistry", 3rd ed., 2007 Elsevier B.V.

[6] Abdelhamied D., W. Albalawi, N. S. Nisar, A. Abdel-Aty, S. Alsaeed, M. Abdelhakem, Mixed Chebyshev and Legendre polynomials differentiation matrices for solving initial-boundary value problems, Aims Mathematics. 8(10), 24609-24631 (2023)

[7] M. Gamal, M. A. Zaky, M. El-Kady, M. Abdelhakem, Chebyshev polynomial derivative-based spectral tau approach for solving high-order differential equations, Comp. Appl. Math., 43, 412 (2024).

[8] Mobarak H. M., E. M. Abo-Eldahab, R. Adel, M. Abdelhakem, MHD 3D nanofluid flow over nonlinearly stretching/shrinking sheet with nonlinear thermal radiation: Novel approximation via Chebyshev polynomials' derivative pseudo-Galerkin method, Alex. Eng. J., 102, 119-131 (2024).

[9] Ulfah S, S A Awalludin and Wahidin: "Advection-diffusion model for the simulation of air pollution distribution from a point source emission", IOP Conf. Series: Journal of Physics: Conf. Series 948 (2018), doi :10.1088/1742-6596/948/1/012067

[10] Pramod Kumar and Maithili Sharan: "An analytical model for dispersion of pollutants from a continuous source in the atmospheric boundary layer", proceeding the royal society, Mathematical, Physical & Engineering Sciences, http://rspa.royalsocietypublishing.org/content/suppl/2009

[11] Sarbjit Singh, Zulfequar Ahmad & Umesh C. Kothyari: "Mixing coefficients for longitudinal and vertical mixing in the near field of a surface pollutant discharge", 2010, Journal of Hydraulic Research 48:1, 91-99, DOI: 10.1080/00221680903566117

[12] Nieuwstadt F. T. M., and van Ulden, A. P. (1978). A numerical study on the vertical dispersion of passive contaminants from a continuous source in the atmospheric surface layer. Atmos. Environ., 12, 2119-2124.

[13] Michael Heisel and Marcelo Chamecki: "On the Departure from Monin–Obukhov Surface Similarity and Transition to the Convective Mixed Layer", Boundary-Layer Meteorology (2024) 190:28 https://doi.org/10.1007/s10546-024-00870-0

[14] Ragland, K. W., Dennis, R. L., (1975). Point source atmospheric diffusion model with variable wind and diffusivity profiles. Atmos. Environ., 9, 175-189.

[15] Chenning Tong and Khuong X. Nguyen: "Multipoint Monin–Obukhov Similarity and Its Application to Turbulence Spectra in the Convective Atmospheric Surface Layer", 2015, American Meteorological Society, DOI: 10.1175/JAS-D-15-0134.1

[16] Kao, S. K. and Yeh, Y.N. (1979), A note on the effects of stack and inversion heights on diffusion of pollutants in the planetary boundary layer. Atmos. Environ., 13, 873-878.

[17] Peter Baas, Stephan R. de Roode, Geert Lenderink: (The Scaling Behaviour of a Turbulent Kinetic Energy Closure Model for Stably Stratified Conditions), Boundary-Layer Meteorology, 2007, DOI:10.1007/s10546-007-9253-y.

[18] Sukanta Basu and Albert A. M. Holtslag: "Turbulent Prandtl number and characteristic length scales in stably stratified flows: steady-state analytical solutions", Environmental Fluid Mechanics (2021) https://doi.org/10.1007/s10652-021-09820-7

[19] Arya SP (2001) Introduction to micrometeorology. Academic Press, Cambridge, 2nd edition.

[20] Holt, T., Raman, S. (1988). A review and comparative evaluation of multilevel boundary layer parameterizations for first-order and turbulent kinetic energy closure schemes. Rev. Geophys., 26, 761-780.

[21] Bowen Zhou, Yuhuan Li, Kefeng Zhu: "Improved Length Scales for Turbulence Kinetic Energy–Based Planetary Boundary Layer Scheme for the Convective Atmospheric Boundary Layer", 2020, American Meteorological Society, DOI: 10.1175/JAS-D-19-0334.1

[22] Detering, H. W., and Etling, D., (1985). Applications of the $E-\varepsilon$ turbulence model to the atmospheric boundary layer. Boundary Layer meteorology, 33, 69-83.

[23] Beljaars, A. C, M., Walmsley, J. L., and Taylor, P. A. (1987). A mixed spectral finite-difference model for neutrally stratified boundary layer flow over roughness changes and topography. Boundary Layer Meteorol., 38, 273-303.

[24] Xiping Zeng and Yansen Wang: "A k–e Turbulence Model for the Convective Atmosphere", 2020, AMS (www.ametsoc.org/PUBSReuseLicenses), DOI: 10.1175/JAS-D-20-0072.1

[25] Mellor, G. L., and Yamada, T. (1982). Development of a turbulence closure model for geophysical fluid problems. Rev. Geophys., 20, 851-875.

[26] Cara-Lyn Lappen, David Randall, and Takanobu Yamaguchi: "A Higher-Order Closure Model with an Explicit PBL Top", 2010, Journal of The Atmospheric Sciences, vol. 67, American Meteorological Society

[27] Wyngaard, J. C., Cote, O. R., and Rao, K. S. (1974). Modeling the atmospheric boundary Layer. Advan. Geophys., 18A, 193-211. Academic Press. New York.

[28] Wyngaard, J. C., (1975). Modeling the planetary boundary layer-extension to the stable case. Boundary Layer Meteorol., 9, 441-460.

[29] Lumley, J. L., and Khajeh-Nouri, B. (1974). Computational modeling of turbulent transport. Adv. Geophys., 18A, 169-192.

[30] Zeman, O., and Lumley, J. I. (1976). Modeling buoyancy driven mixed layers. J. Atmos. Sci., 33, 1974-1988.

[31] Andre J. C., de Moor, G., Lacarrere, P., Therry, G., and du Vachat, R. (1978). Modeling the 24-hour evolution of the mean turbulent structures of the planetary boundary layer. J. Atmos. Sci., 35, 1861-1883.

[32] Lumley, J. L. (1979). Computational modeling of turbulent flows. Adv. Appl. Mech., 18, 123-176.

[33] Gibson, M. M., and Launder, B. E. (1978). Ground effects on pressure fluctuations in the atmospheric boundary layer. J. Fluid Mech., 86, 491-511.

[34] Wyngaard, J. C. (1982). Boundary layer modeling. In Atmospheric Turbulence and Air Pollution Modeling (F.T.M. Nieuwstadt and H. van Dop. Eds.), pp. 69-106. D. Reidel Pub. Co., Dordrecht, Holland.

[35] Sun, W. Y., and Chang, C. Z. (1986). Diffusion model for a convective boundary layer. Part I. Numerical simulation of convective boundary layer. J. Climate Appl. Meteorol., 25, 1445-1453.

[36] Sun, W. Y. (1989) numerical study of dispersion in the convective boundary layer.

[37] Andren, A. (1990). Evaluation of a turbulence closure scheme suitable for air-pollution applications. J. Appl. Meteorol., 29, 224-239.

[38] Daniela Buske, Marco Túllio Vilhena, Tiziano Tirabassi, Bardo Bodmann: "Air Pollution Steady-State Advection-Diffusion Equation: The General Three-Dimensional Solution", Journal of Environmental Protection, 2012, 3, 1124-1134, doi:10.4236/jep.2012.329131

[39] Weil, J. C. (1988b). Dispersion in the convective boundary layer. In Lectures on Air pollution Modeling (A. Venkatram and J. C. Wyngaard, eds.) pp. 167-227. American Meteorological Society, Boston.

[40] Paolo Zannetti: "Air pollution modelling, theories, computational methods and available software", 2nd ed. 1998, computational mechanics publications, Southampton Boston, Van Nostrand Reinhold, New York.

[41] Smith, F. B. (1968). Conditioned particle motion in a homogeneous turbulent field. Atmos. Environ., 2, 491-508.

[42] Hanna S. r. (1979). Some statistics of Lagrangian and Eulerian wind fluctuations. J. Appl. Meteorol., 18, 518-525.

[43] Legg, B. J., and Raupach, M. R. (1982). Markov-chain simulation of particle dispersion in inhomogeneous flows: The mean drift velocity induced by a gradient in Eulerian velocity variance. Boundary Layer Meteorol., 14, 3-13.

[44] Wilson, J. D., Thurtell, G. W., and Kidd, G. E. (1981a). Numerical turbulence simulation of particle trajectories in inhomogeneous turbulence. I: Systems with constant turbulent velocity scale. Boundary Layer Meteorol., 21, 423-441.

[45] Wilson, J. D., Thurtell, G. W., and Kidd, G. E. (1981b). Numerical turbulence simulation of particle trajectories in inhomogeneous turbulence. II: Systems with constant turbulent velocity scale. Boundary Layer Meteorol., 21, 295-313.

[46] Wilson, J. D., and Sawford, B. L. (1996). Review of Lagrangian stochastic models for trajectories in the turbulent atmosphere. Boundary Layer Meteorol., 78, 191-210.

[47] Thomson, D. J. (1987). Criteria for the selection of the stochastic models of particle trajectories in turbulent flows. J. Fluid Mech., 180, 529-556.

[48] Luhar A. K., and Britter, R. E. (1989). A random walk model for dispersion in inhomogeneous turbulence in a convective boundary layer. Atmos. Environ,, 23, 1911-1924.

[49] Hurley, P., and Physick, W. (1993). A skewed homogeneous Lagrangian particle model for convective conditions. Atmos. Environ., 27A, 619-624.

[50] Sawford, B. L. (1993). Recent developments in the Lagrangian stochastic theory of turbulent dispersion. Boundary Layer Meteorol., 62, 197-215.

[51] Bolster, D., M´eheust, Y., Le Borgne, T., Bouquain, J., & Davy, P. (2014). Modeling preasymptotic transport in flows with significant inertial and trapping effects– 770 the importance of velocity correlations and a spatial markov model. Advances in water resources, 70, 89–103. doi: 10.1016/j.advwatres.2014.04.014

[52] Reid, J. D. (1979). Markov-chain simulations of vertical dispersion in the neutral surface layer for surface and elevated releases. Boundary Layer Meteorol. 16, 3-22.

[53] Hyungwon John Park , Thomas Sherman , Livia S Freire , Guiquan Wang , Diogo Bolster : " Predicting Vertical Concentration Profiles in the Marine Atmospheric Boundary Layer With a Markov Chain Random Walk Model",J Geophys Res Atmos., 2020 16;125(19): doi: 10.1029/2020jd032731.

[54] Hall, C. D. (1975). The simulation of particle motion in the atmosphere by a numerical random-walk model. Quart. J. Roy. Meteorol. Soc., 101, 235-244.

[55] Davis, P. A. (1983). Markov-chain simulation of vertical dispersion from elevated sources into the neutral planetary boundary layer. Boundary Layer Meteorol., 26, 355-376.

[56] Luhar A. K., and Rao, K. S. (1993). Random-walk model studies of the transport and diffusion of pollutants in katabatic flows. Boundary Layer Meteorol., 66, 395-412.

[57] Nappo, C. J., and Rao, K. S. ((1987). A model study of pure Katabatic flows. Tellus, 39A, 61-71.

[58] Etling, D., Preuss, J., and Wamser, M. (1986). Application of a random walk model to turbulent diffusion in complex terrain. Atmos. Environ., 20, 741-747.

[59] Gross, G., Vogel, H., and Wipperman, F. (1987). Dispersion over and around a steep obstacle for varying thermal stratification- numerical simulations. Atmos. Environ., 21, 483-490.

[60] McNider, R. T., Moran, M. D., and Pielke R. A. (1988). Influence of diurnal and internal boundary layer oscillation on long-range dispersion. Atmos. Environ., 22, 2445-2462.

[61] Segal, M., Pielke, R. A., Arritt, R.W., Moran, D., Yu, C. H., and Henderson, D. (1988). Application of a mesoscale atmospheric dispersion modeling system to the estimation of $SO_2$ concentrations from major elevated sources in southern Florida. Atmos. Environ., 22, 1319-1334.

[62] Yamada, T., and Bunker, S. (1988). Development of a nested grid second moment turbulence closure model and application to the 1982 ASCOT Bruch Crech data simulation. J. Appl. Meteorol., 27, 562-578.

[63] Physick, W. I., and Abbs, D. J., (1991). Modeling of summer-time flow and dispersion in the coastal terrain of southeastern Australia. Mon. Weath. Rev., 119, 1014-1030.

[64] Pielke, R. A., Cotton, W. R., Walko, R. I., Tremback, C. I., Nicholls, M. E., Moran, M. D., Wesley, D. A., Lee, T. J., and Copeland, J. H. (1992). A comprehensive meteorological modeling system-RAMS Meteorol. Atmos. Phys., 49, 69-91.

[65] Physick, W. I., Noonan, J. A., McGregor, J. L., Hurley, P. J., Abbs, D. J., and Manins, P. C. (1993).

LADM-A Lagrangian atmospheric dispersion model. Technical Report No. 24, CSIRO Division of Atmospheric Research,Australia.

[66] Uliasz, M. (1994). Lagrangian particle dispersion modeling in mesoscale applications. In Environmental Modeling II (P. Zannetti ed.). Computational Mechanics Publications. Pp. 71-102.

[67] Boybeyi, Z., Raman, S., and Zannetti, P. (1995). Numerical investigation of possible role of local meteorology in Bhopal gas accident. Atmos. Environ., 29, 479-496.

[68] Moran, M. D., and Pielke, R. A. (1996). Evaluation of mesoscale atmospheric dispersion modeling system with observations from the 1980 Great Plains Mesoscale Tracer Field Experiment. Part I: Datasets and meteorological simulations. J. Appl. Meteorol., 35, 281-307.

[69] Moran, M. D., and Pielke, R. A. (1996b). Evaluation of mesoscale atmospheric dispersion modeling system with observations from the 1980 Great Plains Mesoscale Tracer Field Experiment. Part II: Dispersion simulation. J. Appl. Meteorol., 35, 308-329.

[70] Boyce,W. and Di Prima, R.: 2001, Elementary Differential Equations and Boundary Value Problems, Wiley, New York, 749 pp.Wiley & Sons, USA.

[71] Gryning, S. E. and Lyck, E.: 1984, 'Atmospheric dispersion from elevated source in un urban area: Comparison between tracer experiments and model calculations', J. Clim. Appl. Meteor. 23, 651–654.

[72] Degrazia, G. A.: 1998, 'Modelling dispersion from elevated sources in a planetary boundary layer dominated by moderate convection', Il Nuovo Cim. C 21(3) 345–353.

[73] Peter E. K. and Eckhard P. (1992) Numerical solution of stochastic differential equations. Springer,23.

[74] Hanna S. R. (1989) Confidence Limit for Air Quality Models as Estimated by Bootstrap and Jacknife Resembling Methods", Atom. Environ. 23:1385-1395.